# Implementation and testing of routing algorithms in the distributed Hydrologiska Byråns Vattenbalansavdelning model for mountainous catchments

Hong Li, Stein Beldring and Chong-Yu Xu

## ABSTRACT

The main purpose of this study was to implement and test routing algorithms in the distributed Hydrologiska Byråns Vattenbalansavdelning (HBV) model with the emphasis of obtaining a most suitable routing algorithm for large mountainous catchments. Two routing algorithms were built into the grid-based HBV model and tested on the Losna (11,213 km$^2$) and the Norsfoss (18,932 km$^2$) catchments in central southern Norway. In the first algorithm, runoff is first routed from cell to cell and hydrographs are re-calculated at each cell, and then runoff is routed by the Muskingum–Cunge method in river channels. The second algorithm is a source-to-sink method, which routes runoff of all cells to the catchment outlet as a function of local slope and a calibrated velocity parameter. The routing approaches were compared at different spatial resolutions (i.e. 1, 5 and 10 km) in daily streamflow simulation. Additionally, the elevation band-based semi-distributed model was also compared with the distributed models. The results show that the distributed HBV models are able to perform better than the elevation band-based model, and hillslope routing is crucial in the mountainous catchments. However, incorporating the Muskingum–Cunge channel routing does not add value to the simulation of daily runoff in the mountainous catchments.

**Key words** | distributed modelling, HBV, mountainous catchment, Norway

**Hong Li**
**Chong-Yu Xu**
Department of Geosciences,
University of Oslo,
PO Box 1047 Blindern, 0316 Oslo,
Norway

**Stein Beldring**
Norwegian Water Resources and Energy Directorate,
PO Box 5091,
Majorstua, 0301 Oslo,
Norway

**Chong-Yu Xu** (corresponding author)
Department of Earth Sciences,
Uppsala University,
75236 Uppsala,
Sweden
E-mail: *chongyu.xu@geo.uio.no*

## INTRODUCTION

There are two main aims of simulation models, i.e. to explore the implications under certain assumptions about the nature of the real world system, and to predict the behaviour of the real world system under a set of naturally occurring and/or human induced circumstances (Beven 1989). Hydrological models provide a framework to investigate relations between climate and hydrologic response, and are widely used in flood forecasting (e.g. Beven *et al.* 1984; Refsgaard *et al.* 1988), water resources assessment (e.g. Xu *et al.* 1996; Kizza *et al.* 2013), global and regional scale water balance calculation (e.g. Arnell 1999; Widén-Nilsson *et al.* 2007; Li *et al.* 2013), simulation of hydrological effect of climate and land use change (e.g. Xu *et al.* 2005; Jiang *et al.* 2012; McIntyre *et al.* 2013) and streamflow prediction in ungauged basins (e.g. Xu & Singh 2004; McIntyre *et al.* 2005; Peel & Blöschl 2011). The development of hydrological models has gone through several stages, from input–output black box models, through lumped conceptual models to physically-based (or conceptual) distributed models (Singh 2002). Due to more explicit representation of hydrological processes and larger parameter space, distributed models are expected to perform better than lumped models. However, the value of the distributed modelling approach cannot be highly recognized if the sole objective is to simulate discharge at the catchment outlet (Beven 2001; Wrede *et al.* 2013). This statement is partly limited to past research and data availability as well as the designed model structure (Frankenberger *et al.* 1999; Wagener *et al.* 1999). Although it is difficult to have a 'fully-distributed' model, it is of scientific and practical interest to investigate the value of distributed modelling approach for hydrological simulation.

doi: 10.2166/nh.2013.009

In most distributed hydrological models, runoff generation is considered as vertical process, and water flows in one dimension in river channels. The isolation between the spatially distributed pixels is a fundamental limitation to their use in defining today's model structures (McDonnell 2003). The increasing attention in variable source area runoff generation concepts (Anderson & Burt 1978; Frankenberger *et al.* 1999; McDonnell 2003) shows that the horizontal processes can also contribute to the runoff generation. It is necessary and worthwhile to develop a fully distributed hydrological model system to include the horizontal processes, which are of importance in runoff routing.

In distributed models, routing is usually dealt with in two ways, i.e. cell-to-cell and source-to-sink. The cell-to-cell approach, like the Muskingum method, consists of determining the amount of water that flows from land cells to its neighbor downstream river cell and tracking the water over the river network. Source-to-sink approach is referring to routing from 'cells in which runoff is produced' to the 'watershed outlet cell'. Advantages of cell-to-cell routing include: (1) ease of implementation within distributed models, reasonable results and the explicit accountant of the volume of river water in each cell; (2) hydrograph computation of any land cell of interest; and (3) the volume of river water stored in the cell can be transformed into a fraction of land area covered by surface water or inundation (Arora *et al.* 2001; Gong *et al.* 2009). The main disadvantage is that the performance of cell-to-cell routing is sensitive to the spatial resolution, since this routing method is based on the river network which is extracted from a digital elevation model (DEM) (Gong *et al.* 2009). Unlike the cell-to-cell routing, the source-to-sink method originates from the travel time, which can go back to the time-area unit hydrograph theory. The travel time is the quotient of distance and flow velocity. The distance is the length of flow path, which is easily calculated from DEM. Assuming the time-independent flow velocity parameterized as a function of slope, Gong *et al.* (2009) reported that source-to-sink method gave stable results independent of spatial resolution, while the performance of a linear-reservoir-routing method, which is a typical cell-to-cell method, declined as the spatial resolution became coarser. Additionally, the source-to-sink method was relatively computation effective. Actually, the sensitiveness of the cell-to-cell method is caused by the river network, not the routing method itself. Unlike the source-to-sink methods which only build relationships between all the grids within the catchment and the outlet, the cell-to-cell methods provide opportunities to examine the effects of water movement between the hillslope surfaces by subdividing the hillslope into a series of discrete spatial cells.

In this research, both cell-to-cell routing method and source-to-sink method are incorporated into the Hydrologiska Byråns Vattenbalansavdelning (HBV) model to study the effects of routing on the simulation of daily runoff in large mountainous catchments. The original HBV model used in this study is a semi-distributed daily conceptual rainfall-runoff model that has been developed into many versions focusing on different aspects (Sælthun 1996; Beldring *et al.* 2003; Ehret *et al.* 2008; Wrede *et al.* 2013). In the late 1990s, Lindström *et al.* (1997) and Krysanova *et al.* (1999) made attempts of developing distributed HBV model using sub-basin division and each sub-basin was divided into elevation bands, vegetation and soil classes. Ehret *et al.* (2008) and Götzinger & Bárdossy (2007) published a grid-based distributed HBV model for different purposes respectively. Wrede *et al.* (2013) further compared the grid-based distributed and elevation band-based semi-distributed HBV model in the lowland region of central Sweden. The elevation band-based model was found to be better than the grid-based distributed HBV in terms of discharge simulation. In the above mentioned publications, no details about the routing techniques are discussed.

The main objective of this study is to implement different types of routing methods into a grid-based HBV model and to compare the new model with the semi-distributed HBV model at different spatial resolutions. This study should not only contribute to the overall understanding of the effects of spatial discretization in conceptual rainfall runoff modelling, but also provide an improved modelling tool for flood forecasting and water resources assessment.

## STUDY AREA AND DATA

### Study area

The Glomma catchment, with a basin area of 41,963 km$^2$, is located in central southern Norway, and covers around

15% of the area of Norway (Figure 1). With two main branches, the Glomma River is the longest river and has the largest drainage basin area in Norway. Approximately, 30% of the catchment is situated above 1,000 m above mean sea level and 40% between 500 and 1,000 m above mean sea level. Climate varies considerably along the Glomma River from upper glacial regions in the northwest to the lowlands in the south. The northern part is characterized by lower temperature, more precipitation and more snow than the southern part (Tockner *et al.* 2009) due to the high altitude and the strong North Atlantic Oscillation effects (Skaugen *et al.* 2012). Records (1961–1990) from the meteorological station in Lillehammer (226 m above mean sea level) showed the mean annual temperature is 2.9 °C, ranging from −9.3 to 14.7 °C in January and July, respectively. The mean annual precipitation is 720 mm, of which more than 50% falls as snow. Floods in the lower parts of the Glomma catchment are usually associated with snow melting, heavy precipitation or their combination (Tockner *et al.* 2009). The Losna and Norsfoss catchments lie in the upstream of western and eastern branches and have an area of 11,213 and 18,932 km$^2$, respectively.

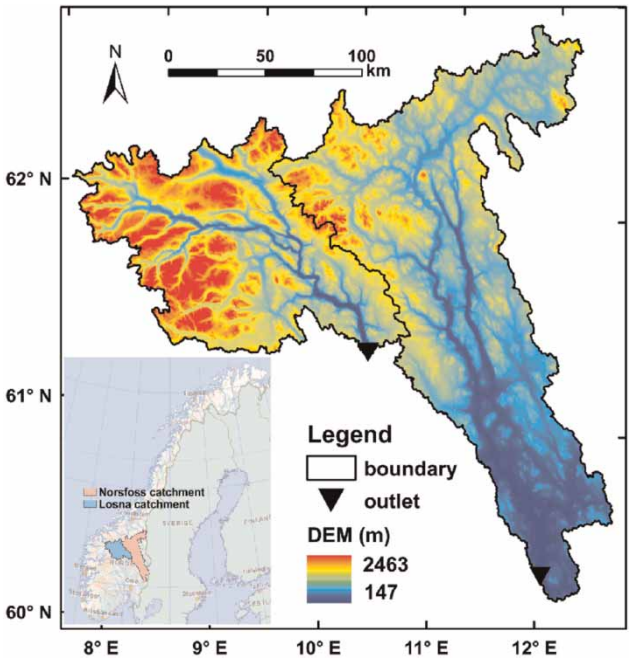


**Figure 1** | The locations and DEM of the Losna and the Norsfoss catchments, Norway.

The mean altitude of the Losna catchment is 1,158 m above mean sea level whereas the mean altitude of the Norsfoss catchment is 732 m above mean sea level. The mean values of slope are 11.8° in the Losna catchment and 6.7° in the Norsfoss catchment.

## Spatial data and processing

Digital map data from the Norwegian Mapping Authority (NMA) were used to determine land use and elevation for each model cell. DEM of horizontal resolution of 25 m was aggregated to 1, 5 and 10 km for comparative purpose. The slope data derived from 25 m DEM by ArcGIS10 were aggregated to 1, 5 and 10 km for the same purpose.

The drainage networks delineation was constructed based on the river Network Scaling Algorithm (NSA) (Fekete *et al.* 2001) at different spatial resolutions. First, we tried to build the river networks based on the original 25 m DEM without success due to many small lakes and bogs being the local sinks, which are very typical in Nordic countries. Then we aggregated the $25 \times 25$ m DEM to $100 \times 100$ m by the mean elevation. Based on the 100 m spatial resolution DEM, flow direction data were constructed according to D8 algorithm by ArcGIS10 for different spatial resolutions. The D8 (deterministic eight-node) algorithm developed by O'Callaghan & Mark (1984) allows flow from a cell to only one of eight nearest neighbors based on the steepest slope. The river network systems at different spatial resolutions were obtained by the NSA method (Fekete *et al.* 2001; Gong *et al.* 2009), and the same accumulation area was used for the threshold value to identify the river cells. The river networks at different resolutions were finally checked by visual inspection according to the digital river networks defined by the Norwegian Water Resources and Energy Directorate (NVE) and manually modified if necessary. The final river networks of three spatial resolutions are shown in Figure 2.

Estimating the channel cross-sectional size is both difficult and essential in river flow routing models. In this research, 93 measurements in the Losna catchment and 111 measurements in the Norsfoss catchment were done from maps. The measured values near the Otta River in the Losna catchment and the Folla River in the Norsfoss catchment were similar to the main channel width

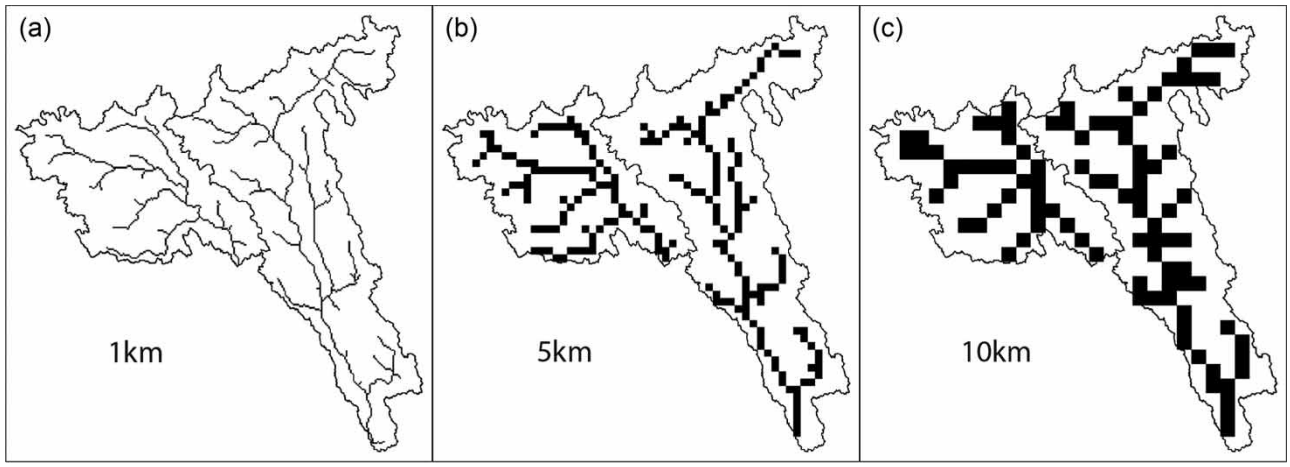


**Figure 2** | The digital river networks of the Losna and Norsfoss catchments at 1, 5 and 10 km horizontal resolutions.

measured in the flooding zone projections carried out by NVE. However, the measured river cross-sectional sizes were not able to be used in the models without preprocessing. In Norway, some lakes, such as Losna and Storsjøen, are very long and crossed by rivers, which would cause large errors near lakes. Additionally, the digital river networks sometimes cannot overlap with the natural river system, which would lead to the use of only a small number of measured river cross sections. To reduce the uncertainty and make full use of the measured data, a method was developed to obtain the river width at different spatial resolutions. First, the digital river networks were ordered in Strahler number (Strahler 1957) and river networks were divided into different sections. Then, the width of one river section was assigned by the mean value of all the river cross sections measured in the responsible local sub-catchment.

The land use data were classified based on vector data at a scale of 1:50,000 (lakes and glaciers) or 1:250,000 (forests and bogs), and all other land use classes were classified as open land or mountainous areas. The potential tree level, which can be thought of as a continuous surface cutting through the landscape along the tree line from NMA, was used to separate areas above and below tree level. The four land classes were subdivided into seven land cover types, i.e. lake, bog, forest, bedrock, heather, subalpine and open land according to the data from a Norwegian Vegetation Atlas (Beldring *et al.* 2003).

## Meteorological and hydrological data

Daily maps of precipitation and temperature at 1 km horizontal resolution for the whole of Norway were used in this study. These datasets are produced by the Norwegian Meteorological Institute using observations of 24-hour mean temperature and accumulated precipitation measured at meteorological stations. The temperature data were interpolated by residual kriging after 'de-trending' to mean sea level, common latitude and common longitude by a linear regression model. For the spatial interpolation of precipitation, the method of triangulation was used with correction for the altitude of grid point using a vertical precipitation gradient of 10% per 100 m difference below 1,000 m above mean sea level and a vertical precipitation gradient of 5% per 100 m difference above 1,000 m above mean sea level (Mohr 2008). These datasets are available from 1960 to date and can be downloaded from www.senorge.no.

The discharge data of the Losna station for the Losna catchment and the Norsfoss station for the Norsfoss catchment obtained from the station network of the Hydrology Department, Norwegian Water Resources and Energy Directorate, were used in the calibration and validation. The daily discharge data were transformed from the original observed stage using Bayesian Rating Curve Fitting method (Petersen-Øverleir *et al.* 2009).

## MODEL DEVELOPMENT AND PARAMETERIZATION

### Model algorithms

The HBV model concepts were developed by the Swedish Meteorological and Hydrological Institute in the early 1970s (Bergström 1976). The main routines are snow accumulation and melting, soil moisture accounting, and runoff generation. A simple degree-day method is used for snowmelt calculation, and the evapotranspiration is calculated based on field capacity and permanent wilting point. The runoff is simulated by two non-linear parallel reservoirs representing the direct discharge and the groundwater response with the spatial distribution of soil saturation controlling the response described by a non-linear distribution function. Additional detailed information of the model used in this study can be found in the references (Sælthun 1996; Lindström *et al.* 1997).

The model performs water balance calculations for every discretized element. The new distributed HBV is also able to simulate the sub-grid variability with fractions of land classes within one element. Outflow from the lake is modeled by a non-linear reservoir based on inflow and storage. Every element has components for accumulation, sub-grid scale distribution and ablation of snow, interception storage, evapotranspiration, ground water storage and runoff response, lake evaporation and glacier mass balance (Beldring *et al.* 2003). Two types of water movements are incorporated to the grid-based HBV model. The first is runoff of landscape cell draining to the next landscape cell until discharging into the river cell, and then runoff is routed by the Muskingum–Cunge method in the river channel. The second is called Network Response Function (NRF) (Gong *et al.* 2009; Li *et al.* 2013), in which runoff of all cells flows to the catchment outlet as a function of local slope and a calibrated water velocity parameter. Details of the method will be discussed in the later sections.

### Parameters and calibration

The parameters were calibrated by a model-independent nonlinear parameter estimation and optimisation package called Parameter ESTimation (PEST). It is frequently used for model calibration in different research fields. It is based on the implementation of the Gauss–Marquardt–Levenberg algorithm, which combines the advantages of the inverse Hessian matrix and the steepest gradient method to allow a fast and efficient convergence towards the best value of objective function. Within the specified ranges of parameters, PEST approaches the global optimized parameter set by minimizing the discrepancies between simulated and observed values in a weighted least square sense (Doherty & Johnston 2003; Wrede *et al.* 2013). Some parameters were fixed, and others with a physically plausible range were calibrated twice. The initial values of the second round were the results of the first round of calibration. All the lakes in the study area were using the same parameter values, and land use parameter values varied for every land use class. The fixed parameters and ranges of calibrated parameters are shown in Table 1.

### Model setups

This study compared six different model setups, including a semi-distributed model, i.e. elevation band-based HBV and a grid-based HBV without routing, and four grid-based distributed HBV models with different routing methods.

#### Semi-distributed models

Two semi-distributed models include the following. (1) The HBV with 10 elevation bands for each catchment, called LBand. The meteorological data were extracted for every elevation band from 1 km grid meteorological data and the mean values were used as the input of every elevation band. (2) The first grid-based HBV divides each catchment into square grid cells, and runoff generation is performed in every grid. The catchment outlet discharge is the sum-up of all the catchment cells runoff. This model setup is called Direct0 in this research.

#### Distributed models

According to the routing in the hillslope and the river cells, four grid-based distributed models are defined as follows. (1) DirectM only considers distributed routing in the rivers, and runoff generation is performed in every grid.

**Table 1** | The parameter meanings and calibrated minimum (Min) and maximum (Max) or fixed values in PEST estimation. The MannR was only used in the Muskingum–Cunge channel routing method. SSV was only used in the source-to-sink routing method, NRF

| | | | | Min | Max |
|---|---|---|---|---|---|
| | **Parameters** | **Explanation** | **Unit** | **Or fixed value** | |
| General | CORR_RAIN | Precipitation correction for gauge error | – | 1.0 | |
| | CORR_SNOW | Additional correction for snow | – | 1.0 | |
| | LAPSE_DRY | Temperature lapse rate in dry days | d | 0.0 | |
| | LAPSE_WET | Temperature lapse rate in wet days | d | 0.0 | |
| | SSV | Water velocity parameter | m/s | 7 | 50 |
| Lake | TMEMORY | Lake temperature memory | d | 30 | |
| | KLAKE | Rating curve constant | – | 1E-4 | 1.0 |
| | DLEVEL | Rating curve saddle point | m | 0.0 | |
| | NLAKE | Rating curve exponent | – | 1E-4 | 200 |
| Land uses | INTER_MAX | Maximum interception storage | m | 1E-4 | 0.03 |
| | ACC_T | Snow accumulation temperature | °C | 0.0 | |
| | SMELT_T | Snow melt temperature | °C | –2.0 | 3.5 |
| | SMELTR | Temperature index of snow melting rate | m/°C | 1E-5 | 0.1 |
| | IMELTR | Temperature index of glacier ice melting rate | m/°C | 0.005 | |
| | FRREEZR | Refreezing coefficient of water in snow | – | 0.01 | |
| | MAX_REL | Maximum free water in snow pack | – | 0.08 | |
| | FC | Field capacity | m | 0.05 | 3.5 |
| | FCDEL | Maximum evaporation efficiency | – | 1.0 | |
| | BETA | Shape coefficient of soil moisture | – | 0.1 | 10 |
| | INFMAX | Infiltration capacity | m | 1.0 | |
| | KUZ | Upper zone recession coefficient | – | 1E-6 | 1.0 |
| | ALFA | Upper zone nonlinear drainage coefficient | – | 0.1 | 2.5 |
| | PERC | Percolation from upper zone to lower zone | – | 0.001 | 0.2 |
| | KLZ | Lower recession coefficient | – | 0.001 | 1.0 |
| | DRAW | Draw up coefficient from lower zone to soil moisture | – | 0.0 | |
| Lake and land use | EPOT_PAR | Potential evaporation capacity | m/d | 1E-6 | 0.002 |
| | MannR | Manning roughness coefficient | – | 0.001 | 0.3 |

The runoff is summed at the respective river cell and is routed by the Muskingum–Cunge method between the river cells. The river channel shape is assumed to be rectangle. When the Courant number is greater than one, the output discharge is equal to input discharge, which means no routing. Details of Muskingum–Cunge method can be seen from, for example, Todini (2007). (2) Drain0 only considers the distributed hillslope routing without routing in the river, which is calculated following Equations (1) and (2). First, the runoff generation subroutine runs in the most upslope cells, and the generated runoff is added to the soil moisture storage and subsequently to groundwater storage in the downslope landscape cell. Second, runoff from the downslope cell is determined by the runoff from the upslope cell and the local net precipitation. Third, runoff generation routine performs from the upslope cells to the downslope cells until the runoff discharges into the river cell. (3) DrainM considers both the distributed hillslope and river routing. (4) The source-to-sink method is NRF adopted from Gong *et al.* (2009). This method considers the distributed hillslope and river routing by the same procedure, and routes runoff of all cells to the catchment outlet using Equations (3) and (4). The six model setups are summarized in Table 2.

$$SM_j = \mathrm{Net}P_j + \sum_{i=1}^{n} R_i \quad (1)$$

$$R = RU + RL \quad (2)$$

where *SM:* soil moisture storage; Net*P*: net precipitation; *R:* grid total runoff; *RU*: grid runoff from the upper zone;

**Table 2** | Definitions of model setups. Grid models were tested at three spatial resolutions

| Setups | Explanation |
|---|---|
| LBand | Semi-distributed model with 10 elevation bands |
| Direct0 | Grid-based semi-distributed model without routing |
| DirectM | Grid-based distributed model with distributed routing in the river |
| Drain0 | Grid-based distributed model with distributed routing in the hillslope cells |
| DrainM | Grid-based distributed model with distributed routing in the hillslope cells and the river cells |
| NRF | Grid-based distributed model with distributed routing in the hillslope cells and the river cells by time delay calculated by Equations (3) and (4) |

$RL$: grid runoff from the lower zone; $i$, $j$: grid index; $n$: the number of the upslope cell of the $j$th cell.

$$V_i = V\sqrt{S_i} \tag{3}$$

$$t = \sum_{i=1}^{n} \frac{l_i}{V_i} \tag{4}$$

where $S_i$: $i$th grid slope in the flow path; $V$: calibrated water velocity parameter; $V_i$: grid velocity as a function of $V$ and slope length; $l_i$: $i$th grid slope length in the flow path; $t$: travel time of one grid.

## RESULTS

The six models defined in the previous chapter were calibrated during 1981–1990 and validated during 1991–2010 both for the Losna and Norsfoss stations. The models based on square grid were calibrated and validated at 1, 5 and 10 km horizontal resolutions, respectively. The Nash–Sutcliffe efficiency (NSE) (Nash & Sutcliffe 1970) and relative mean error (RME) were used as the criteria for model performance. Their formulas are shown in Equations (5) and (6).

$$\mathrm{NSE} = 1 - \frac{\sum_{i=1}^{n}(O_i - S_i)^2}{\sum_{i=1}^{n}(O_i - \overline{O_i})^2} \tag{5}$$

$$\mathrm{RME} = \frac{\sum_{i=1}^{n}(S_i - O_i)}{\sum_{i=1}^{n} O_i} \times 100 \tag{6}$$

where $O_i$ and $S_i$ are the observed and simulated flows, respectively; $i$ is the time series index, and $n$ is the total number of time steps.

As shown in Table 3, the RME of all the models are less than 3% with an exception in the Losna catchment at the 10 km spatial resolution for the Direct0 and NRF models. Only the results of NSE are discussed in the following sections since RME is small for all the models, as can be seen in Table 3.

The five grid-based distributed model setups could be grouped to two categories – 'Drain' and 'Direct' – according to whether or not involving land routing process, which means water interactions between the landscape cells. Direct0, DirectM and NRF are in the 'Direct' category. The NRF model does not consider the water interactions between landscape cells, but only the time delay from the individual grid to the catchment outlet. Drain0 and DrainM are in the 'Drain' category.

**Table 3** | The relative mean error (RME) of models of the validation period (1991–2010). The RME for LBand is –1.41 for the Losna station and –1.09 for the Norsfoss station (not shown in the table)

| Catchment | Resolution (km) | Direct0 | DirectM | Drain0 | DrainM | NRF |
|---|---|---|---|---|---|---|
| Losna | 1 | 1.34 | 1.34 | 1.60 | 1.02 | 1.30 |
| | 5 | 1.79 | 1.79 | −2.58 | −0.33 | 1.79 |
| | 10 | **− 7.63** | −1.45 | −1.36 | −1.30 | **− 7.62** |
| Norsfoss | 1 | 1.25 | 1.23 | 0.77 | 0.01 | 1.24 |
| | 5 | −0.80 | −0.80 | 2.53 | −0.20 | −0.80 |
| | 10 | −1.22 | −0.72 | 0.44 | 0.14 | −1.22 |

## Model comparison

The results of NSE are shown in Figure 3. The following can be seen from the figure. (1) All the six model setups in Norsfoss catchment performed better than in the Losna catchment. That is mainly due to the location of the Losna catchment in the higher elevation and with lower quality of precipitation and temperature input than the Norsfoss catchment. Additionally, the Losna is more regulated than the Norsfoss catchment and the HBV model structure in our research is for natural conditions. (2) The models are similar within the two model categories, and the 'Drain' models are better than the 'Direct' models. In the 'Direct' category, NRF is the best. DirectM and Direct0 are similar both in the Losna and the Norsfoss catchments. In the 'Drain' category, Drain0 and DrainM are similar. The 'Drain' models are better (above 0.838 in the Losna catchment and 0.914 in the Norsfoss catchment for the validation) than the 'Direct' models (below 0.797 in the Losna catchment and 0.844 in the Norsfoss catchment for the validation). (3) The small differences made by the Muskingum–Cunge channel routing method both in the 'Direct' or 'Drain' category shows that the channel routing does not add values in the daily flow simulation in the mountainous catchments in Norway.

## Spatial resolution effects

Sensitivity of distributed models to spatial resolution is an important characteristic of model robustness. The grid based models were compared in Figure 4 for three spatial resolutions, i.e. 1, 5 and 10 km.

The following can be seen from Figure 4. (1) Generally the models perform better in the Norsfoss catchment than in the Losna catchment. The 'Drain' models are better than 'Direct' models at three spatial resolutions, which probably imply that the water interaction between the landscape elements is the main process determining the discharge response in cold and mountainous catchments, even at large scale. (2) The models are still similar at three spatial resolutions within the 'Drain' and 'Direct' category with small fluctuations. In the 'Drain' category, the largest difference between Drain0 and DrainM was 0.02 occurring in the Norsfoss catchment at the 5 km spatial resolution for the validation, and in the Losna catchment at the 1 and 5 km spatial resolutions for the validation. The three 'Direct' models are also similar except for DirectM being 0.881 for calibration and 0.831 for validation in the Losna catchment at 10 km spatial resolution whereas Direct0 and NRF are below 0.8 both in the calibration and the validation. (3) The NSE values of Direct0, DirectM and NRF show a

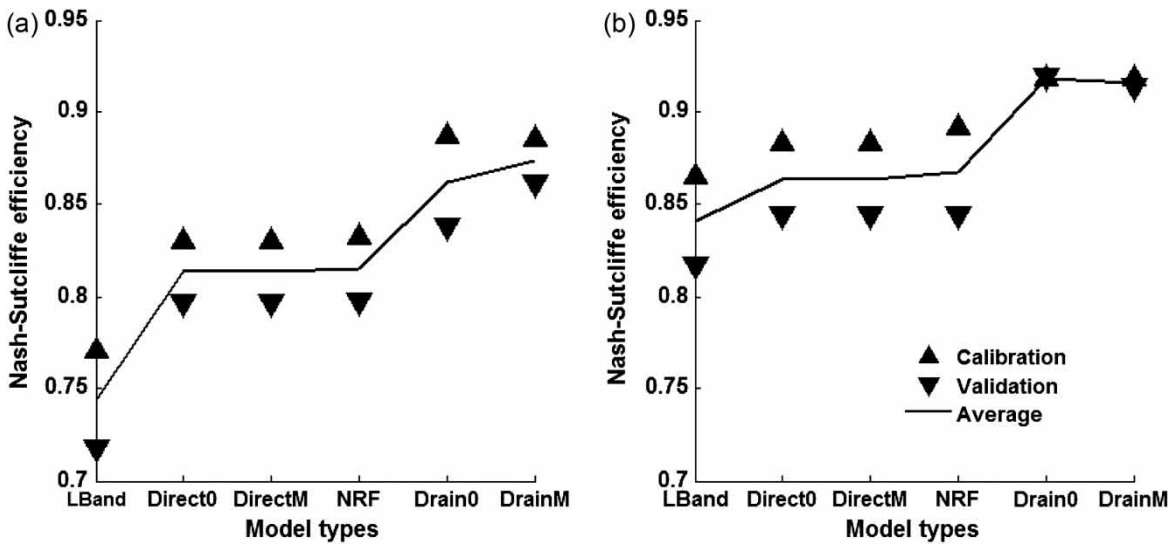


**Figure 3** | NSE of LBand and five grid-based model setups at 1 km spatial resolution in the Losna (a) and Norsfoss (b) catchments for the calibration and the validation. Average is the mean Nash–Sutcliffe efficiency of the calibration and the validation.

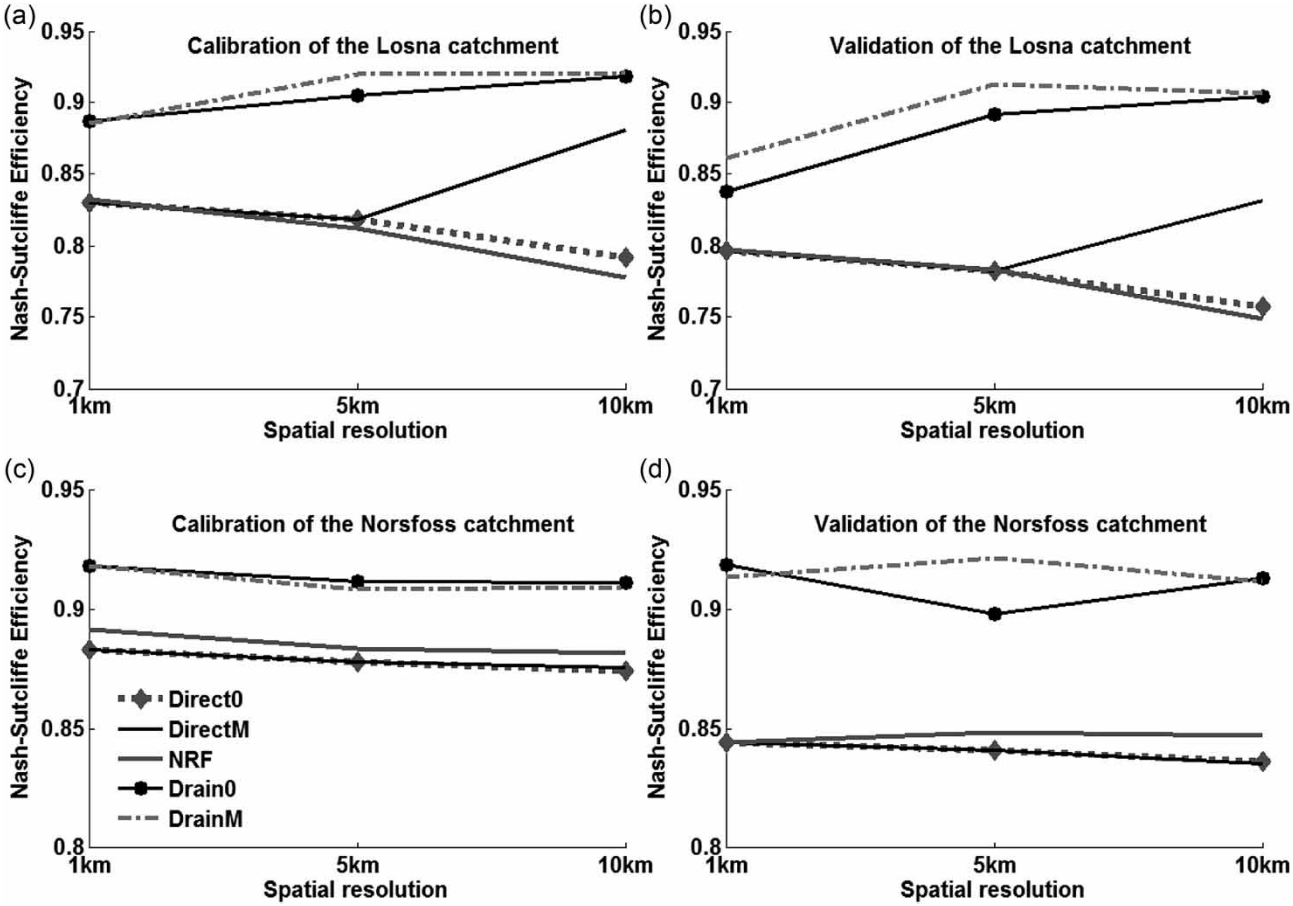


**Figure 4** | The NSE in the Losna and Norsfoss catchments for calibration and validation in five grid-based model setups. (a) The calibration of the Losna catchment; (b) the validation of the Losna catchment; (c) the calibration of the Norsfoss catchment; and (d) the validation of the Norsfoss catchment.

decreasing trend with increasing spatial resolution with one exception in the Losna catchment at 10 km spatial resolution in DirectM model, whereas this trend of 'Drain' models is not clear.

It is also interesting to investigate why in the Losna catchment the 'Drain' models perform better at the 5 and 10 km spatial resolutions than at the 1 km spatial resolution, however, the reasons are not clear. The model performance is a systematic and compromised result of the input data, model structure and parameter values. Coarser resolution leads to low quality input data, which is expected to result in decreasing model performance. The degree of regulation in the Losna catchment is relatively higher (with regulation capacities of 13.66%) than that in the Norsfoss catchment (with regulation capacities of 8.57%) based on the discharge data from 1961 to 1990. The simulation results as reflected by the NSE do not seem to be affected much in the Norsfoss catchment, and are slightly affected in the Losna catchment. The higher elevation and lower quality of precipitation and temperature input in the Losna catchment might be the main reason for the different model performances in these two catchments. Nevertheless, the results of this study show that different spatial resolutions (1, 5 and 10 km) do not result in significant difference in terms of discharge simulations. More studies need to be performed in the on-going research in order to generalize the findings presented in this study.

## DISCUSSION

One strong advantage of NRF is that the method can tell the travel time of every grid to the catchment outlet,

which can provide information about the discharge response at the catchment outlet (Gong *et al.* 2009). The effects of time delay of runoff can be examined by the discharge sensitivity to the water velocity parameter, and the result is shown in Figure 5. The calibrated NSE was not sensitive when the water velocity parameter was greater than 17 m/s in the Losna catchment and 22 m/s in the Norsfoss catchment. However, in the Norsfoss catchment the decreasing trend is slightly larger than that in the Losna catchment when the water velocity parameter is larger than 30 m/s. This slightly larger decreasing trend is due to the longer travel time in the Norsfoss catchment than in the Losna catchment because of the difference in the catchment shape, slope, land cover and soil. The better performance of NRF than Direct0 in the Norsfoss catchment (Figure 4) also demonstrates the longer travel time.

The calibrated water velocity parameter is 24 m/s in the Losna catchment and 26 m/s in the Norsfoss catchment, and these two values were used in 5 and 10 km NRF routing. Although the calibrated water velocity parameter of the Losna catchment is smaller than that in the Norsfoss catchment, the Losna catchment has a much faster response than the Norsfoss catchment (Figure 6). Figure 6 shows that most of the runoff would flow out within 2 days, which is reasonable due to the high slope. Therefore, the time delay caused by routing in the river networks is difficult to present in daily models. However, the flow velocity is only simplified as a function of a calibrated water velocity parameter and slope

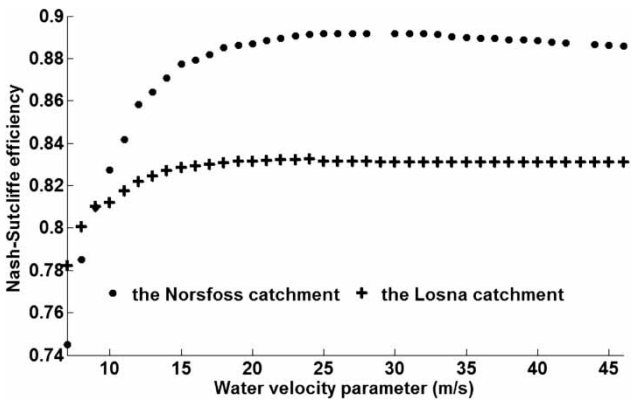


**Figure 5** | The calibrated results of the source-to-sink method, NRF, at different values of water velocity parameter.

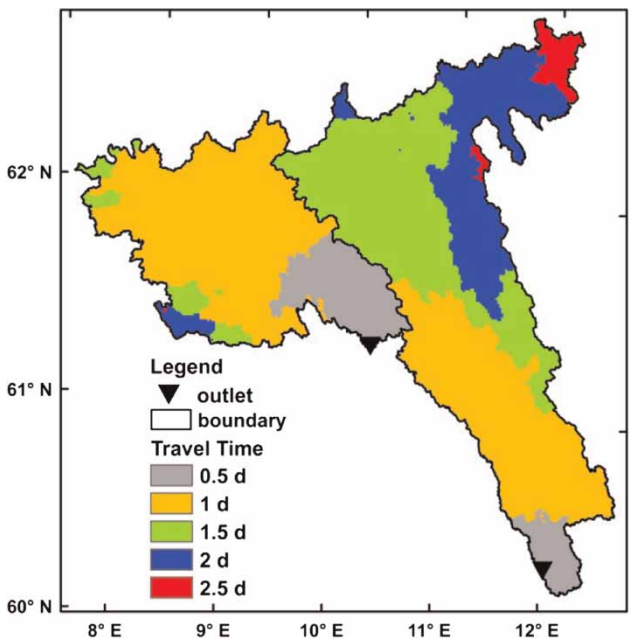


**Figure 6** | The travel times of two catchments. The calibrated water velocity parameter is 24 m/s in the Losna catchment and 26 m/s in the Norsfoss catchment. Note that the water velocity parameter is not the natural flow velocity. The travel time is calculated according to Equations (3) and (4). The travel time is also related to the slope, and some inconsistent mosaics were caused by small local slope.

due to the lack of detailed and high quality data of soil and vegetation, etc. The error caused by this simplification can be reduced by calibrating the velocity parameter as did in this study instead of estimating them as a prior. The slight improvements made by NRF in the two catchments imply that the time delay exists in the catchments, and no further improvements by the Muskingum–Cunge channel routing indicate that the time delay is not mainly caused by channel routing. In contrast, the significant improvements from the 'Direct' to the 'Drain' models show that the time delay exists between the landscape elements.

The different model setups are based on the same HBV concepts with the same input data, and are calibrated by the same automatic calibration package. The differences are caused only by the routing algorithms. Direct0 only considers the horizontal distribution of input data; Drain0 considers the horizontal distribution of input data and the water interactions between the landscape cells; DirectM considers the horizontal distribution of input data and the distributed routing in the river networks; DrainM considers

the horizontal distribution of input data, the water interactions between the landscape cells, and the distributed routing in the river network; NRF considers the horizontal distribution of input data and the time delay between the grid cells and the catchment outlet. In the development of distributed hydrological models, the same runoff generation processes as in lumped models can still be used, and the problem arises as to how to make the distributed elements communicate with each other.

In this research, the hydrological models are only evaluated according to the daily river flow simulation in terms of NSE and RME. In regulated catchments, even well structured hydrological models for natural condition are not easily able to give good simulation. Besides, the good fitness in the observed discharge cannot promise good simulation in other hydrological variables. Even the models produce similar discharge, other hydrological variables vary significantly and huge different prediction in climate changing scenarios (Boorman & Sefton 1997; Jiang *et al.* 2007). It will be necessary to compare these models according to the simulation of other hydrological state variables or fluxes, such as groundwater storage, soil moisture, evapotranspiration or their exchange in the on-going research.

## CONCLUSIONS

In this paper, a grid-based distributed HBV model with two widely used routing methods, a cell-to-cell method with hillslope routing and river routing, and a source-to-sink method were tested in the two sub-catchments of the Glomma basin at 1, 5 and 10 km spatial resolutions. The grid-based distributed HBV models were able to perform remarkably better than the semi-distributed elevation band-based model. The results show that the main discharge response was controlled by the water interactions between landscape cells and taking that into account can improve the daily flow simulation significantly. Additionally, we do not find clear trend of model performances in the model category including the water interactions between the landscape cells, whereas model performance without this interactions shows decreasing trend with coarser resolution. Introducing the Muskingum–Cunge channel routing method does not further improve the modelling result in these two mountainous catchments in daily flow simulation at various spatial resolutions. Further studies are needed involving more methods and catchments in order to provide generalized conclusions and guidelines on the flow routing methods in distributed hydrological modelling.

## ACKNOWLEDGEMENTS

We are grateful to Dr Lu Li at University of Oslo and Dr Lebing Gong at Uppsala University for helping with the NRF routing methods. This study was partly funded by the Research Council of Norway through the research project JOINTINDNOR (project number 203867). All the hydrological data were provided by Norwegian Water Resources and Energy Directorate.

## REFERENCES

Anderson, M. G. & Burt, T. P. 1978 Toward more detailed field monitoring of variable source areas. *Water Resour. Res.* **14** (6), 1123–1131.

Arnell, N. W. 1999 A simple water balance model for the simulation of streamflow over a large geographic domain. *J. Hydrol.* **217**, 314–335.

Arora, V., Seglenieks, F., Kouwen, N. & Soulis, E. 2001 Scaling aspects of river flow routing. *Hydrol. Proc.* **15** (3), 461–477.

Beldring, S., Engeland, K., Roald, L. A., Sælthun, N. R. & Voksø, A. 2003 Estimation of parameters in a distributed precipitation-runoff model for Norway. *Hydrol. Earth Syst. Sci.* **7** (3), 304–316.

Bergström, S. 1976 Development and application of a conceptual runoff model for Scandinavian catchments. SMHI Report RHO 7, Norrköping, 134 pp.

Beven, K. J. 1989 Changing ideas in hydrology – The case of physically-based models. *J. Hydrol.* **105** (1–2), 157–172.

Beven, K. J. 2001 Dalton Medal Lecture: How far can we go in distributed hydrological modelling? *Hydrol. Earth Syst. Sci.* **5** (1), 1–12.

Beven, K. J., Kirkby, M. J., Scoeld, N. & Tagg, A. F. 1984 Testing a physically-based flood forecasting model (TOPMODEL) for three UK catchments. *J. Hydrol.* **69**, 119–143.

Boorman, D. B. & Sefton, C. 1997 Recognising the uncertainty in the quantification of the effects of climate change on hydrological response. *Clim. Change* **35** (4), 415–434.

Doherty, J. & Johnston, J. M. 2003 Methodologies for calibration and predictive analysis of a watershed model. *J. Am. Water Resour. Assoc.* **39** (2), 251–265.

Ehret, U., Götzinger, J., Bárdossy, A. & Pegram, G. G. S. 2008 Radar-based flood forecasting in small catchments, exemplified by the Goldersbach catchment, Germany. *Int. J. River Basin Manage.* **6** (4), 323–329.

Fekete, B. M., Vörösmarty, C. J. & Lammers, R. B. 2001 Scaling gridded river networks for macroscale hydrology: Development, analysis, and control of error. *Water Resour. Res.* **37** (7), 1955–1967.

Frankenberger, J. R., Brooks, E. S., Walter, M. T., Walter, M. F. & Steenhuis, T. S. 1999 A GIS-based variable source area hydrology model. *Hydrol. Proc.* **13** (6), 805–822.

Gong, L., Widen-Nilsson, E., Halldin, S. & Xu, C. Y. 2009 Large-scale runoff routing with an aggregated network-response function. *J. Hydrol.* **368** (1–4), 237–250.

Götzinger, J. & Bárdossy, A. 2007 Comparison of four regionalisation methods for a distributed hydrological model. *J. Hydrol.* **333**, 374–384.

Jiang, T., Chen, Y. D., Xu, C. Y., Chen, X. & Singh, V. P. 2007 Comparison of hydrological impacts of climate change simulated by six hydrological models in the Dongjiang Basin, South China. *J. Hydrol.* **336** (3–4), 316–333.

Jiang, S., Ren, L., Yong, B., Fu, C. & Yang, X. 2012 Analyzing the effects of climate variability and human activities on runoff from the Laohahe basin in northern China. *Hydrol. Res.* **43** (1–2), 3–13.

Kizza, M., Guerrero, J.-L., Rodhe, A., Xu, C. Y. & Ntale, H. K. 2013 Modelling catchment inflows into Lake Victoria: Regionalisation of the parameters of a conceptual water balance model. *Hydrol. Res.* **44** (5), 789–808, doi:10.2166/nh.2012.152.

Krysanova, V., Bronstert, A. & Müller-Wohlfeil, D.-I. 1999 Modelling river discharge for large drainage basins: from lumped to distributed approach. *Hydrol. Sci. J.* **44** (2), 313–331.

Li, L., Ngongondo, C. S., Xu, C. Y. & Gong, L. 2013 Comparison of the global TRMM and WFD precipitation datasets in driving a large-scale hydrological model in southern Africa. *Hydrol. Res.* **44** (5), 770–788, doi:10.2166/nh.2012.175.

Lindström, G., Johansson, B., Persson, M., Gardelin, M. & Bergström, S. 1997 Development and test of the distributed HBV-96 hydrological model. *J. Hydrol.* **201** (1–4), 272–288.

McDonnell, J. J. 2003 Where does water go when it rains? Moving beyond the variable source area concept of rainfall-runoff response. *Hydrol. Proc.* **17** (9), 1869–1875.

McIntyre, N., Ballard, B., Bruen, M., Bulygina, N., Buytaert, W., Cluckie, I., Dunn, S., Ehret, U., Ewen, J., Gelfan, A., Hess, T., Hughes, D., Jackson, B., Kjeldsen, T., Merz, R., Park, J-S., O'Connell, E., O'Donnell, G., Oudin, L., Todini, E., Wagener, T. & Wheater, H. 2013 Modelling the hydrological impacts of rural land use change. *Hydrol. Res.* in press, doi:10.2166/nh.2013.145.

McIntyre, N., Lee, H., Wheater, H., Young, A. & Wagener, T. 2005 Ensemble predictions of runoff in ungauged catchments. *Water Resour. Res.* **41** (12), W12434.

Mohr, M. 2008 New Routines for Gridding of Temperature and Precipitation Observations for 'seNorge. no'. No. 08/2008, Norwegian Meteorological Institute, Norway.

Peel, M. C. & Blöschl, G. 2011 Hydrological modelling in a changing world. *Prog. Phys. Geog.* **35** (2), 249–261.

Nash, J. E. & Sutcliffe, J. V. 1970 River flow forecasting through conceptual models part I – A discussion of principles. *J. Hydrol.* **10** (3), 282–290.

O'Callaghan, J. F. & Mark, D. M. 1984 The extraction of drainage networks from digital elevation data. *Comput. Vis. Graph. Image Proc.* **28**, 323–344.

Petersen-Øverleir, A., Soot, A. & Reitan, T. 2009 Bayesian rating curve inference as a streamflow data quality assessment tool. *Water Resour. Manage.* **23** (9), 1835–1842.

Refsgaard, J. C., Havnø, K., Ammentorp, H. C. & Verwey, A. 1988 Applications of hydrological models for flood forecasting and flood control in India and Bangladesh. *Adv. Water Resour.* **11**, 101–105.

Skaugen, T., Stranden, H. B. & Saloranta, T. 2012 Trends in snow water equivalent in Norway (1931–2009). *Hydrol. Res.* **43** (4), 489–499.

Singh, V. P. 2002 *Mathematical Models of Small Watershed Hydrology and Applications*. Water Resources Publication, Littleton, CO, USA.

Strahler, A. N. 1957 Quantitative analysis of watershed geomorphology. *Trans. Am. Geophys. Union* **38** (6), 913–920.

Sælthun, N. R. 1996 The Nordic HBV Model. No. 7, Norwegian Water Resources and Energy Directorate, Norway.

Tockner, K., Uehlinger, U. & Robinson, C. T. 2009 *Rivers of Europe*. Academic Press, London, UK.

Todini, E. 2007 A mass conservative and water storage consistent variable parameter Muskingum-Cunge approach. *Hydrol. Earth Syst. Sci.* **11** (5), 1645–1659.

Wagener, T., Boyle, D. P., Lees, M. J., Wheater, H. S., Gupta, H. V. & Sorooshian, S. 1999 A framework for development and application of hydrological models. *Hydrol. Earth Syst. Sci.* **5** (1), 13–26.

Widén-Nilsson, E., Halldin, S. & Xu, C. Y. 2007 Global water-balance modelling with WASMOD-M: Parameter estimation and regionalisation. *J. Hydrol.* **340**, 105–118.

Wrede, S., Seibert, J. & Uhlenbrook, S. 2013 Distributed conceptual modelling in a Swedish lowland catchment: a multi-criteria model assessment. *Hydrol. Res.* **44** (2), 318–333.

Xu, C. Y. & Singh, V. P. 2004 Review on regional water resources assessment models under stationary and changing climate. *Water Resour. Manage.* **18** (6), 591–612.

Xu, C. Y., Seibert, J. & Halldin, S. 1996 Regional water balance modelling in the NOPEX area: development and application of monthly water balance models. *J. Hydrol.* **180**, 211–236.

Xu, C. Y., Widén-Nilsson, E. & Halldin, S. 2005 Modelling hydrological consequences of climate change – progress and challenges. *Adv. Atmospher. Sci.* **22** (6), 789–797.

First received 10 January 2013; accepted in revised form 11 June 2013. Available online 17 August 2013